Robustness of superposition states evolving under the influence of a thermal reservoir

J. S. Sales[1] and N. G. de Almeida[2]
[1]*UnUCET - Universidade Estadual de Goiás, 75132-903, Anápolis (GO), Brazil*
[2]*Instituto de Física, Universidade Federal de Goiás, 74001-970, Goi ânia (GO), Brazil*

(Received 1 October 2010; published 27 June 2011)

We study the evolution of superposition states under the influence of a reservoir at zero and finite temperatures in cavity quantum electrodynamics aiming to know how their purity is lost over time. The superpositions studied here are composed of coherent states, orthogonal coherent states, squeezed coherent states, and orthogonal squeezed coherent states, which we introduce to generalize the orthogonal coherent states. For comparison, we also show how the robustness of the superpositions studied here differs from that of a qubit given by a superposition of zero- and one-photon states.

DOI: 10.1103/PhysRevA.83.062121 PACS number(s): 03.65.Yz, 42.50.Dv

I. INTRODUCTION

Coherent superposition is at the heart of quantum mechanics and finds applications in a number of technological advances. For example, in quantum information and quantum computation, coherent superposition is one fundamental property of a qubit necessary to perform quantum Fourier transform, quantum phase estimation, quantum search, Deutsch algorithm, quantum cryptography, and dense coding [1]. However, as is well known, it is impossible to completely isolate a qubit from its environment, which destroys the coherence and drives the superposition to an incoherent mixture [2]. Since different superpositions in general will suffer different effects from the surroundings, it is important to know which superposition is more robust compared to the others when the environment is taken into account. In this paper, we model the qubit by superposition states composed of several states usually employed in both theoretical [3–6] and experimental studies [7–9], and then we comparatively study their robustness against a thermal environment through the linear entropy. The superposition states studied here are the squeezed coherent-state superposition (SCSS), coherent-state superposition (CSS), orthogonal squeezed coherent-state superposition (OSCS), and orthogonal coherent-state superposition (OCSS). For comparison, we also plot the linear entropy of the zero- and one-Fock superposition state, or qubit (QBIT), since the zero and one states are ordinarily taken as the computational basis. To study the evolution of these states, we consider the cavity quantum electrodynamics (QED) scenario, where important experiments were recently carried out [8], including the monitoring of purity losses of a CSS [7]. Statistical properties of an ideal, i.e., lossless SCSS were widely studied [10], and schemes for engineering Hamiltonians leading to arbitrary squeezed states in ideal high-Q cavity QED were discussed in Refs. [11–14]. Different from these previous works, the SCSS studied here takes into account the reservoir at finite temperature, and it is straightforwardly generalized to generate CSS, OSCS, and OCSS as particular cases.

It is to be noted that robustness of entanglement, which is also a key property for quantum information tasks, was introduced for any state of a composite system composed by any finite number of local subsystems of finite dimension [15]. In Ref. [16], the authors study the robustness of generalized multiqubit Greenberger-Horne-Zeilinger-type states, and in Ref. [17], the dynamics of multipartite entanglement under the influence of decoherence for various environments is investigated. Recently, an experimental work leading with robustness of bipartite Gaussian entangled beams propagating in lossy channels was reported for the simplest case of two light beams [18]. Entanglement robustness has also been studied by several authors in the cavity QED domain [19–21].

This paper is organized as follows. In Sec. II we introduce the model to include the environment and derive the evolution of the SCSS under a thermal reservoir. In Sec. III we study the time evolution of the linear entropy considering the initial states in the superpositions mentioned above, and in Sec. IV we present our conclusions.

II. THE MODEL

For modeling the system and reservoir, we will use, as usual, the following Hamiltonian:

$$H = \hbar\omega a^\dagger a + \sum_k \hbar\omega_k b_k^\dagger b_k + \sum_k \hbar(\lambda_k a^\dagger b_k + \lambda_k^* a b_k^\dagger), \quad (1)$$

where $a^\dagger$ and a are, respectively, the creation and annihilation operators for the cavity mode of frequency ω, and $b_k^\dagger$ and b_k are the analogous operators for the kth reservoir oscillator mode, whose corresponding frequency and coupling are ω_k and λ_k, respectively.

A. SCSS evolution under thermal reservoir

The SCSS evolution under a thermal reservoir can be obtained, using the approach of characteristic functions [22] for example. Let us delineate the main steps involved. First, we calculate the characteristic function in the symmetrical order (C), then we calculate the Wigner function, and finally, we obtain the linear entropy. For convenience, we first calculate the characteristic function in the normal order (C_N), which is related to the symmetrical C function by

$$C(\eta,\eta^*,t) = C_N(\eta,\eta^*,t)e^{-\frac{|\eta|^2}{2}}. \quad (2)$$

In the Heisenberg picture, C_N reads

$$C_N(\eta,\eta^*,t) = \mathrm{tr}\{\rho_{AR}(0)\exp[\eta a^\dagger(t)]\exp[\eta^* a(t)]\}, \quad (3)$$

where tr denotes trace on both mode and reservoir variables, η is a c number, and $\rho_{AR}(0)$ is the density operator for the whole system at time $t=0$, composed of the cavity mode field (system A) prepared in the SCSS state,

$$a|\xi,\alpha\rangle + b|\xi,-\alpha\rangle, \tag{4}$$

and the reservoir (R). The Wigner W function is given by the two-dimensional Fourier transform of the characteristic C function,

$$W(\gamma,\gamma^*,t) = \frac{1}{\pi^2}\int d^2\eta e^{\eta^*\gamma-\eta\gamma^*}C(\eta,\eta^*,t). \tag{5}$$

For the Hamiltonian model given by Eq. (1), the solution of the Heisenberg equations for $a(t)$ and $b_k(t)$ operators can be obtained in the Wigner-Weisskopf approximation, considering the reservoir as Markovian [6,22,23], allowing us to write

$$a(t) = w(t)a(0) + \sum_k v_k(t)b_k(0), \tag{6}$$

where $w(t) = \exp[-(\frac{\Gamma}{2}+i\omega)t]$ and $v_k(t) = \frac{i\lambda\exp[-(\frac{\Gamma}{2}+i\omega)t]-\exp(\omega_k t)}{\frac{\Gamma}{2}+i(\omega_k-\omega)}$, and with $\Gamma = 2\pi D(\omega)|\lambda(\omega)|^2$ being the damping constant of the cavity mode field. Here, $D(\omega)$ is the density of modes inside the cavity taken at the system frequency ω, and $\lambda_k \to \lambda(\omega)$ is the coupling between the system and the reservoir, also taken at the system frequency ω. For a white-noise reservoir, $D(\omega)|\lambda(\omega)|^2$ turns to be a constant, and for high-Q cavities, Γ is experimentally around 10^2 s^{-1}, accounting for a cavity Q factor around 10^8 [7].

Once we have Eq. (6), we can obtain Eqs. (3)–(5) for the SCSS, whose initial density operator reads

$$\rho(0) = \sum_{j,k=1}^{2} b_{jk}|\xi,\alpha_k\rangle\langle\xi,\alpha_j|, \tag{7}$$

where $\alpha_1=\alpha$, $\alpha_2=-\alpha$, and the coefficients b_{jk} are obtained from Eq. (4).

When Eq. (7) is inserted in Eq. (2), the characteristic C function will contain four terms. To obtain the W function for the SCSS into a lossy cavity, we focus our attention on the following representative term of the C function:

$$C_{jk}(\eta,\eta^*,t) = \mathrm{tr}\, b_{jk}|\xi,\alpha_k\rangle\langle\xi,\alpha_j|\exp[\eta a^\dagger(t)-\eta^* a(t)], \tag{8}$$

which can be used to compose Eq. (2) performing the sum $\sum_{j,k=1}^{2} C_{jk}(\eta,\eta^*,t)$. If we now substitute $a(t)$ from Eq. (6) in Eq. (2), and assume the reservoir at a finite absolute temperature, we obtain

$$\begin{aligned}
C(\eta,\eta^*,t) &= \mathrm{tr}\Big[\rho_{AR}(0)e^{\eta[w^*(t)a^\dagger+\sum_k v_k^*(t)b_k^\dagger]}e^{-\eta^*[w(t)a+\sum_k v_k(t)b_k]}e^{-\frac{|\eta|^2}{2}}\Big]\\
&= e^{-\frac{|\eta|^2}{2}}\mathrm{tr}\Big[\rho_A(0)e^{\eta w^*(t)a^\dagger}e^{-\eta^* w(t)a}\Big]\mathrm{tr}\Big[\rho_R(0)e^{\eta\sum_k v_k^*(t)b_k^\dagger}e^{-\eta^*\sum_k v_k(t)b_k}\Big]\\
&= e^{-\frac{|\eta|^2}{2}}\mathrm{tr}\Big[\rho_A(0)e^{\eta w^*(t)a^\dagger}e^{-\eta^* w(t)a}\Big]\mathrm{tr}\left[\prod_k\int d^2\beta_k\frac{e^{\frac{-|\beta_k|^2}{\langle n_k\rangle}}}{\pi\langle n_k\rangle}|\beta_k\rangle\langle\beta_k|e^{\eta v_k^*(t)b_k^\dagger}e^{-\eta^* v_k(t)b_k}\right]\\
&= e^{-\frac{|\eta|^2}{2}}\mathrm{tr}\left[\rho_A(0)e^{\eta w^*(t)a^\dagger}e^{-\eta^* w(t)a}\prod_k e^{-|\eta|^2|v_k(t)|^2\langle n_k\rangle}\right]\\
&= e^{-\frac{|\eta|^2}{2}}\mathrm{tr}\Big[\rho_A(0)e^{\eta w^*(t)a^\dagger}e^{-\eta^* w(t)a}e^{-|\eta|^2\sum_k|v_k(t)|^2\langle n_k\rangle}\Big],
\end{aligned} \tag{9}$$

where we have used $\rho_R(0) = \prod_k\int d^2\beta_k\frac{e^{\frac{-|\beta_k|^2}{\langle n_k\rangle}}}{\pi\langle n_k\rangle}|\beta_k\rangle\langle\beta_k|$ for the reservoir characterized by the mean number occupation $\langle n_k\rangle$ in the kth mode using the coherent states $|\beta_k\rangle$ [22,24]. Using Eq. (7), we can write, for the representative term of $C(\eta,\eta^*,t)$,

$$\begin{aligned}
C_{jk}(\eta,\eta^*,t) &= b_{jk}e^{-(\epsilon+\frac{1}{2})|\eta|^2}\langle\xi,\alpha_j|\exp[\eta w^*(t)a^\dagger]\exp[-\eta^* w(t)a]|\xi,\alpha_k\rangle\\
&= b_{jk}e^{-(\epsilon+\frac{1}{2})|\eta|^2}\langle\alpha_j|\exp[\eta w^*(t)(\mu^* a^\dagger-\nu^* a)]\exp[-\eta^* w(t)(\mu a-\nu a^\dagger)]|\alpha_k\rangle,
\end{aligned} \tag{10}$$

where we have put $a(0)=a$ and $\sum_k|v_k(t)|^2\langle n_k\rangle=\epsilon$. Using the Baker-Campbell-Hausdorff formula $e^{A+B}=e^Ae^Be^{-\frac{1}{2}[A,B]}=e^Be^Ae^{\frac{1}{2}[A,B]}$, with $[A,[A,B]]=0$, we can write

$$\begin{aligned}
C_{jk}(\eta,\eta^*,t) = b_{jk}e^{-(\epsilon+\frac{1}{2})|\eta|^2}&\exp\big[-\tfrac{1}{2}\eta^2 w^{*2}(t)\mu^*\nu^*-\tfrac{1}{2}\eta^{*2}w^2(t)\mu\nu+\eta w^*(t)\mu^*\alpha_j^*\big]\\
&\times\exp[-\eta^* w(t)\mu\alpha_k]\langle\alpha_j|\exp[-\eta w^*(t)\nu^* a+\eta^* w(t)\nu a^\dagger]|\alpha_k\rangle.
\end{aligned} \tag{11}$$

Using $\langle\alpha|a = (\frac{\alpha}{2}+\frac{\partial}{\partial\alpha^*})\langle\alpha|$ and its conjugate, with $|\alpha\rangle = \exp(-\frac{1}{2}|\alpha|^2+\alpha a^\dagger)|0\rangle$, we have, after derivation,

$$\begin{aligned}
C_{jk}(\eta,\eta^*,t) = b_{jk}e^{-(\epsilon+\frac{1}{2})|\eta|^2}&\exp\big[-\tfrac{1}{2}\eta^2 w^{*2}(t)\mu^*\nu^*-\tfrac{1}{2}\eta^{*2}w^2(t)\mu\nu+\eta w^*(t)\mu^*\alpha_j^*-\eta^* w(t)\mu\alpha_k\big]\\
&\times\exp\big[-\tfrac{1}{2}(|\alpha_j|^2+|\alpha_k|^2)\big]\langle 0|\exp\{[-\eta w^*(t)\nu^*+\alpha_j^*]a\}\exp\{[\eta^* w(t)\nu+\alpha_k]a^\dagger\}|0\rangle,
\end{aligned} \tag{12}$$

or, after rearranging the terms and using again $|\alpha\rangle = \exp(-\frac{1}{2}|\alpha|^2+\alpha a^\dagger)|0\rangle$,

$$\begin{aligned}
C_{jk}(\eta,\eta^*,t) = b_{jk}e^{-(\epsilon+\frac{1}{2})|\eta|^2}&\exp\big[-\tfrac{1}{2}\eta^2 w^{*2}(t)\mu^*\nu^*-\tfrac{1}{2}\eta^{*2}w^2(t)\mu\nu\big]\exp\big[\eta w^*(t)\mu^*\alpha_j^*-\eta^* w(t)\mu\alpha_k-\tfrac{1}{2}(|\alpha_j|^2+|\alpha_k|^2)\big]\\
&\times\exp\big\{\tfrac{1}{2}|[-\eta w^*(t)\nu^*+\alpha_j^*]|^2+\tfrac{1}{2}|[\eta^* w(t)\nu+\alpha_k]|^2\big\}\langle-\eta^* w(t)\nu+\alpha_k|\eta^* w(t)\nu+\alpha_j\rangle.
\end{aligned} \tag{13}$$

Finally, using the identity $\langle\beta|\alpha\rangle = \exp(-\frac{1}{2}|\beta|^2 - \frac{1}{2}|\alpha|^2 + \beta^*\alpha)$, we can write

$$C_{jk}(\eta,\eta^*,t) = b_{jk}e^{-(\epsilon+\frac{1}{2})|\eta|^2}\exp\left[-\tfrac{1}{2}\eta^2 w^{*2}(t)\mu^*\nu^* - \tfrac{1}{2}\eta^{*2}w^2(t)\mu\nu\right]\exp\left[\eta w^*(t)\mu^*\alpha_j^* - \eta^* w(t)\mu\alpha_k - \tfrac{1}{2}(|\alpha_j|^2+|\alpha_k|^2)\right]$$
$$\times\exp[-|\eta w(t)\nu|^2 - \eta w^*(t)\nu^*\alpha_k + \eta^* w(t)\nu\alpha_j^* + \alpha_j^*\alpha_k], \tag{14}$$

which can be written as

$$C_{jk}(\eta,\eta^*,t) = b_{jk}\langle\alpha_j|\alpha_k\rangle\exp\Big\{-\tfrac{1}{2}\eta^2 w^*(t)^2\mu^*\nu^* - \tfrac{1}{2}\eta^{*2}w(t)^2\mu\nu + \eta w^*(t)(\mu^*\alpha_j^* - \nu^*\alpha_k).$$
$$-\eta^* w(t)(\mu\alpha_k - \nu\alpha_j^*) - |\eta|^2\big[|w(t)\nu|^2 + \epsilon + \tfrac{1}{2}\big]\Big\}. \tag{15}$$

1. W function

For obtaining the W_{jk} representative term of the W function, we must solve the integral in Eq. (5) with the aid of Eq. (15) as

$$W_{jk}(\gamma^*,\gamma,t) = \frac{b_{jk}}{\pi^2}\langle\xi,\alpha_j|\xi,\alpha_k\rangle\int d^2\eta\exp\Big\{-\frac{1}{2}\eta^2 w^{*2}(t)\mu^*\nu^* - \frac{1}{2}\eta^{*2}w^2(t)\mu\nu + \eta[w^*(t)(\mu^*\alpha_j^* - \nu^*\alpha_k) - \gamma^*] - \eta^*[w(t)(\mu\alpha_k - \nu\alpha_j^*) - \gamma] - |\eta|^2\Big[|w(t)\nu|^2 + \epsilon + \frac{1}{2}\Big]\Big\}, \tag{16}$$

which can be integrated using [25,26]

$$\int d^2\lambda e^{-K|\lambda|^2 - \frac{1}{2}L_1\lambda^{*2} - \frac{1}{2}L_2\lambda^2 - M_1\lambda^* - M_2\lambda} = \frac{\pi}{\sqrt{K^2 - L_1L_2}}\exp\left[\frac{KM_1M_2 - \frac{1}{2}(L_1M_2^2 + L_2M_1^2)}{K^2 - L_1L_2}\right], \tag{17}$$

whose result is a real function provided that $K^2 - L_1L_2 > 0$. If we now identify $K = |w(t)\nu|^2 + \epsilon + \frac{1}{2}$, $L_1 = w^2(t)\mu\nu \equiv L$, $L_2 = L^*$, $M_1 = w(t)(\mu\alpha_k - \nu\alpha_j^*) - \gamma \equiv M_{kj}$, and $M_2 = -M_{jk}^*$, then the representative term of the W function can be written as

$$W_{jk}(\gamma,\gamma^*,t) = \frac{b_{jk}}{\pi}\frac{\langle\xi,\alpha_j|\xi,\alpha_k\rangle}{\sqrt{K^2 - LL^*}}\times\exp\left[-\frac{KM_{jk}M_{kj}^* + \frac{1}{2}(LM_{kj}^{*2} + L^*M_{jk}^2)}{K^2 - LL^*}\right], \tag{18}$$

which can be used to write $W = \sum_{j,k=1}^{2}W_{jk}(\eta,\eta^*,t)$. Note that the condition $K^2 - LL^* > 0$ is always satisfied for the Wigner function.

2. OSCS and OCSS

The squeezed coherent states $|\xi,\alpha\rangle$ and $|\xi,-\alpha\rangle$ are not orthogonal to each other. However, we can define a state $|\xi,\alpha\rangle_\perp = A|\xi,\alpha\rangle + B|\xi,-\alpha\rangle$ which is orthogonal to $|\xi,\alpha\rangle$. Keeping A and B real numbers, we must have

$$(\langle\xi,\alpha|A + \langle\xi,-\alpha|B)|\xi,\alpha\rangle = 0, \tag{19}$$

thus resulting in $A = -\frac{1}{2}\frac{\exp(-|\alpha|^2)}{\sqrt{\sinh(|\alpha|^2)\cosh(|\alpha|^2)}}$ and $B = -\frac{1}{2}\frac{\exp(|\alpha|^2)}{\sqrt{\sinh(|\alpha|^2)\cosh(|\alpha|^2)}}$, such that

$$|\xi,\alpha\rangle_\perp = \frac{-\exp(-|\alpha|^2)|\xi,\alpha\rangle + \exp(|\alpha|^2)|\xi,-\alpha\rangle}{2\sqrt{\sinh(|\alpha|^2)\cosh(|\alpha|^2)}}, \tag{20}$$

which can be rewritten as Eq. (4) with a similar density operator given by Eq. (7). Note that the OCSS emerges as a particular case when $\xi = 0$, i.e., $|\xi = 0,\alpha\rangle_\perp = |\alpha\rangle_\perp$, which is orthogonal to the coherent state $|\alpha\rangle$ [27].

III. LINEAR ENTROPY

To study purity loss in the above-mentioned states, we focus our attention on time evolution of the linear entropy for the SCSS, since the other states result as particular cases. The linear entropy in quantum information theory is defined as $E = 1 - \mathrm{tr}\,\rho^2(t)$, where $\rho(t)$ is the density operator for the system at time t. According to its definition, linear entropy has a minimum for pure states, $\rho = \rho^2$, and it is expected, therefore, that states evolving in time such that their entropy remains minimum are more useful for quantum processing tasks. For our purposes, we rewrite the linear entropy using the Wigner function W as

$$E = 1 - \pi\int d^2\gamma W^2(\gamma,t). \tag{21}$$

The linear entropy for the SCSS is obtained by solving Eq. (21) using Eq. (18):

$$E = 1 - \sum_{j,k=1}^{2}\sum_{r,s=1}^{2}b_{jk}b_{rs}\frac{\langle\xi,\alpha_j|\xi,\alpha_k\rangle\langle\xi,\alpha_r|\xi,\alpha_s\rangle}{2\sqrt{D}}$$
$$\times\exp\left[-\frac{2K|w(t)|^2(B_{jk}B_{kj}^* + B_{rs}B_{sr}^*) + Lw(t)^{*2}(B_{kj}^{*2} + B_{sr}^{*2}) + L^*w(t)^2(B_{jk}^2 + B_{rs}^2)}{2D}\right]$$
$$\times\exp\left\{-\frac{[L(R_{jk} + R_{sr})^2 + L^*(Q_{jk} + Q_{rs})^2] - K(Q_{jk} + Q_{rs})(R_{jk} + R_{sr})}{2D^2}\right\}, \tag{22}$$

where $D = K^2 - LL^*$, $B_{kj} = (\mu\alpha_k - \nu\alpha_j^*)$, $Q_{jk} + Q_{rs} = Kw(t)B_{jk} + Lw(t)^* B_{kj}^* + Kw(t)B_{rs} + Lw(t)^* B_{sr}^*$, and $R_{jk} + R_{rs} = L^* w(t)B_{jk} + Kw(t)^* B_{kj}^* + L^* w(t)B_{rs} + Kw(t)^* B_{sr}^*$. Note that when $t \to \infty$, then $w(t) \to 0$ and $\sqrt{D} = K = (\epsilon + \frac{1}{2})$, with $\epsilon \to \langle n_k \rangle$. Therefore, large times $E \to 1 - \frac{1}{2(\langle n_k\rangle + \frac{1}{2})} = \frac{2\langle n_k\rangle}{2\langle n_k\rangle + 1}$. By writing $\langle n_k \rangle = \frac{1}{\exp(\beta\hbar\omega) - 1}$, with β being the inverse of the reservoir temperature, we obtain $E = \frac{2}{\exp(\beta\hbar\omega)+1}$, which is the entropy for a thermalized Gibbs state [28], as expected.

3. QBIT

For comparison, we also plot the linear entropy for an equally weighted superposition of a qubit (QBIT) which lies in a two-dimensional Hilbert space. The linear entropy for the QBIT is quickly obtained correctly from the density operator [22]. If we define $|\Psi\rangle = \frac{1}{\sqrt{2}}(|0\rangle + |1\rangle)$, then

$$\rho(t) = \frac{1}{2}\left\{\left[e^{-(2\bar{n}+1)\Gamma t} + \frac{(1 - e^{-(2\bar{n}+1)\Gamma t})}{2\bar{n}+1}\right]|0\rangle\langle 0| + \left[2 - e^{-(2\bar{n}+1)\Gamma t} - \frac{2\bar{n}(1 - e^{-(2\bar{n}+1)\Gamma t})}{2\bar{n}+1}\right]|1\rangle\langle 1| + e^{-(\bar{n}+\frac{1}{2})\Gamma t}(|0\rangle\langle 1| + |1\rangle\langle 0|)\right\}, \tag{23}$$

where Γ is the damping constant of the cavity mode field appearing in Eq. (6), such that from $E = 1 - \mathrm{tr}\,\rho^2(t)$ we get

$$\rho^2(t) = \frac{1}{4}\left[\left\{e^{-(\bar{n}+\frac{1}{2})\Gamma t} + \left[e^{-(2\bar{n}+1)\Gamma t} + \frac{2\bar{n}(1 - e^{-(2\bar{n}+1)\Gamma t})}{2\bar{n}+1}\right]^2\right\}|0\rangle\langle 0| + \left\{e^{-(\bar{n}+\frac{1}{2})\Gamma t} + \left[2 - e^{-(2\bar{n}+1)\Gamma t} - \frac{2\bar{n}(1 - e^{-(2\bar{n}+1)\Gamma t})}{2\bar{n}+1}\right]^2\right\}|1\rangle\langle 1| + f(t)(|0\rangle\langle 1| + g(t)|1\rangle\langle 0|)\right], \tag{24}$$

where $f(t)$ is an unimportant function for our purposes, since tracing out the density operator variables, we find

$$E = 1 - \frac{1}{4}\left\{2e^{-2(\bar{n}+\frac{1}{2})\Gamma t} + \left[e^{-(2\bar{n}+1)\Gamma t} + \frac{2\bar{n}(1 - e^{-(2\bar{n}+1)\Gamma t})}{2\bar{n}+1}\right]^2 + \left[2 - e^{-(2\bar{n}+1)\Gamma t} - \frac{2\bar{n}(1 - e^{-(2\bar{n}+1)\Gamma t})}{2\bar{n}+1}\right]^2\right\}. \tag{25}$$

From the above equation, we note that for $\bar{n} = 0$, the linear entropy is null for either $t = 0$ or $t \to \infty$. This is explained by noting that the linear entropy will be null whenever the state is a pure one. As we are beginning with pure states at $t = 0$, the linear entropy starts from zero, and since at zero absolute temperature, the final state is the (pure) vacuum state, the entropy becomes zero. However, for large $\bar{n}$, the final state is no longer the vacuum state, and the entropy no longer vanishes. To compare the linear entropy evolving in time for these different states, we adopt the following criteria. Since the coherence of a

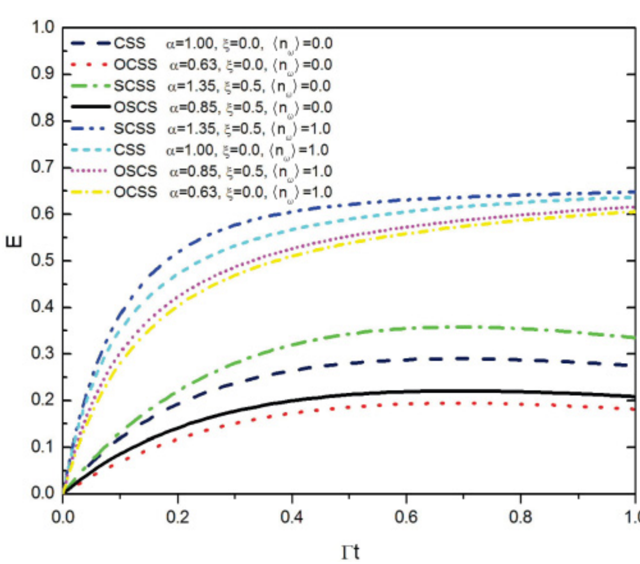

FIG. 1. (Color online) Linear entropy at zero and finite temperature for CSS, OCSS, SCSS and OSCS. The parameters α and ξ were chosen to ensure that all the states have the same mean photon number $\overline{n} = 0.8$.

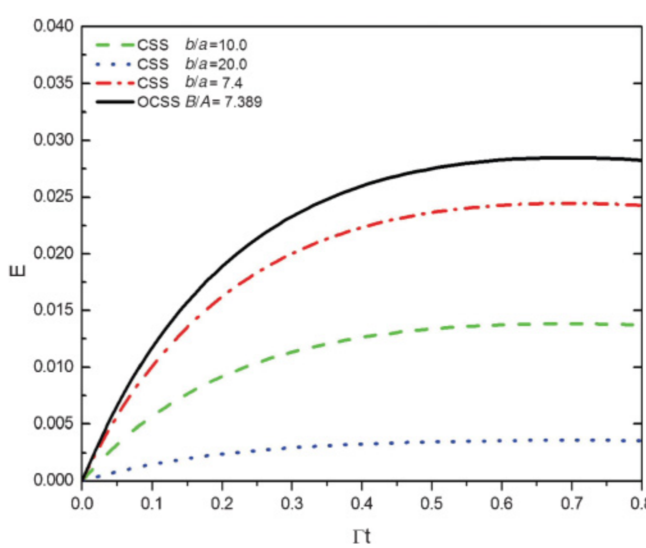

FIG. 2. (Color online) Linear entropy at zero temperature for OCSS and CSS with $\alpha = 1$, considering the different amplitude of probabilities for CSS. For OCSS, $B/A = 7.389\,1$ (solid line), and for CSS, $b/a = 7.4$ (dash-dotted line), $b/a = 10$ (dashed line), and $b/a = 20$ (dotted line).

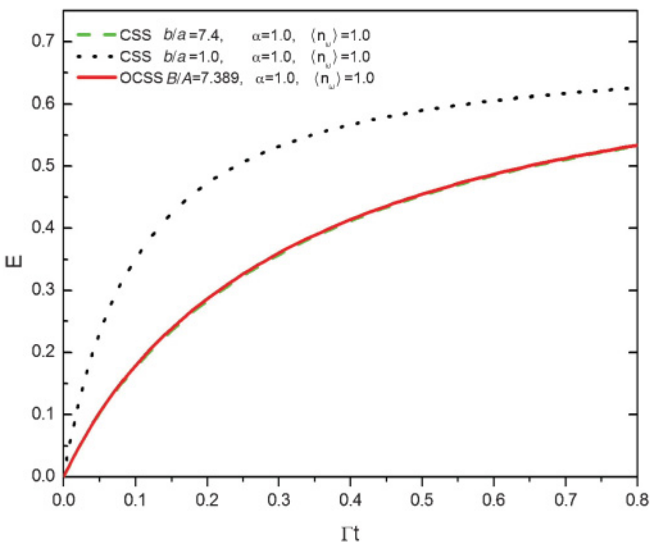

FIG. 3. (Color online) Linear entropy considering the reservoir with a mean occupation number $\overline{n}_\omega = 1.0$ for an equally weighted CSS (dot) and for CSS with $b/a = 7.4$ (dash) and OCSS with $B/A = 7.3891$ (solid). Here we used $\alpha = 1$.

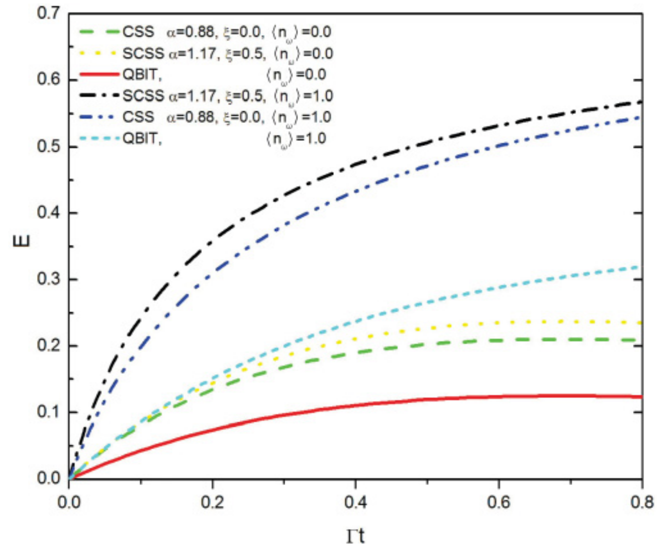

FIG. 4. (Color online) Linear entropy at zero and finite temperature for SCSS, CSS, and QBIT. The parameters α and ξ were chosen to ensure that all the states have the same mean photon number $\overline{n} = 0.5$ and are equally weighted.

superposition is sensitive to the mean photon number, we first fixed the same initial mean photon number for each superposition state. In Fig. 1 we plot the linear entropy for the SCSS, OSCS, OCSS, and CSS for zero and finite temperatures. As expected, temperature effects drastically reduce purity, although not at the same rate for each superposition. Actually, these figures show that the OCSS loses purity more slowly compared to the others, thus suggesting that it is more advantageous to encode information on this state when the environment cannot be neglected. However, a more accurate study reveals why the slower rate happens: since the probability amplitudes for OCSS are defined as $A = -\frac{\exp(-|\alpha|^2)}{2\sqrt{\cosh(|\alpha|^2)\sinh(|\alpha|^2)}}$ and $B = \frac{\exp(|\alpha|^2)}{2\sqrt{\sinh(|\alpha|^2)\cosh(|\alpha|^2)}}$, then for large mean photon number $|\alpha|^2$, the amplitude A vanishes, and hence the initial state is nearly the coherent state. As is well known, coherent states are robust under thermal-reservoir evolution, mainly at zero temperature, when it loses excitation coherently.

This point is made clear in Figs. 2 and 3, which compare the linear entropy for OCSS with that of a CSS at zero and finite temperature, considering the different amplitude of probabilities. Note from these figures that when $B/A \to 0$, the behavior of the linear entropy for both OCSS and CSS becomes similar. Figure 4 includes the time dependence of the linear entropy at zero and finite temperature for an equally weighted qubit, which has initially a mean photon number 0.5. Note that the equally weighted qubit possesses more robustness compared to the other equally weighted superposition states studied here, provided that all superposition states start with the same mean photon number.

IV. CONCLUSION

In this paper, we investigate the robustness of several superposition states when evolving under a thermal reservoir at zero and finite temperature by means of the linear entropy. The superpositions studied here were the coherent state, the orthogonal coherent state (OCSS), the squeezed coherent state, and the orthogonal squeezed coherent state, which we have introduced to generalize the OCSS, and the qubit given by the zero- and one-photon state. Through the analysis of the linear entropy, we show that, fixing the same mean photon number for initial superposition states, the OCSS is the most robust against the unavoidable interaction with the surrounding, losing purity at a rate much slower than the other states even when the finite temperature is taken into account. This slower rate shown by the OCSS, although impressive at first sight, is explained when we look at the corresponding probability amplitudes: since one component of the superposition contributes very little, the OCSS is nearly a coherent state, which loses excitation coherently at zero temperature, and at lower rates at finite temperatures.

ACKNOWLEDGMENTS

The authors acknowledge financial support from the Brazilian agency CNPq. This work was performed as part of the Brazilian National Institute of Science and Technology (INCT) for Quantum Information. J.S.S. thanks Dr. W. B. Cardoso and Dr. G. C. Colherinhas for helping with the plots.

[1] M. A. Nielsen and I. L. Chuang, *Quantum Computation and Quantum Information* (Cambridge University Press, Cambridge, 2000).

[2] H. Carmichael, *An Open System Approach to Quantum Optics* (Springer-Verlag, Berlin, 1993).

[3] N. G. de Almeida, R. Napolitano, and M. H. Y. Moussa, Phys. Rev. A **62**, 010101R (2000).
[4] M. Yang and Z.-L. Cao, Phys. A **366**, 243 (2006).
[5] N. G. de Almeida, R. Napolitano, and M. H. Y. Moussa, Phys. Rev. A **80**, 033801 (2009).
[6] I. P. de Queirós, W. B. Cardoso, and N. G. de Almeida, J. Phys. B **40**, 21 (2007).
[7] J. M. Raimond, M. Brune, and S. Haroche, Phys. Rev. Lett. **79**, 1964 (1997).
[8] J. M. Raimond, M. Brune, and S. Haroche, Rev. Mod. Phys. **73**, 565 (2001).
[9] L. Davidovich, A. Maali, M. Brune, J. M. Raimond, and S. Haroche, Phys. Rev. Lett. **71**, 2360 (1993).
[10] *Horizons on World Physics*, edited by T. F. George and F. A. Henke, Theoretical Physics, Vol. 243, Pt. 2 (Nova Science, New York, 2002).
[11] C. J. Villas-Bôas, N. G. de Almeida, R. M. Serra, and M. H. Y. Moussa, Phys. Rev. A **68**, 061801(R) (2003).
[12] N. G. de Almeida, R. M. Serra, C. J. Villas-Bôas, and M. H. Y. Moussa, Phys. Rev. A **69**, 35802 (2004).
[13] F. O. Prado, N. G. de Almeida, M. H. Y. Moussa, C. J. Villas-Bôas, Phys. Rev. A **73**, 43803 (2006).
[14] R. M. Serra, C. J. Villas-Bôas, N. G. de Almeida, and M. H. Y. Moussa, Phys. Rev. A **71**, 045802 (2005).
[15] G. Vidal and R. Tarrach, Phys. Rev. A **59**, 141 (1999).
[16] Z.-X. Man, Y.-J. Xia, and N. B. An, Phys. Rev. A **78**, 064301 (2008).
[17] A. R. R. Carvalho, F. Mintert, and A. Buchleitner, Phys. Rev. Lett. **93**, 230501 (2004).
[18] F. A. S. Barbosa, A. S. Coelho, A. J. de Faria, K. N. Cassemiro, A. S. Villar, P. Nussenzveig, and M. Martinelli, Nature Photon. **4**, 858 (2010).
[19] L. Aolita, D. Cavalcanti, A. Acín, A. Salles, M. Tiersch, A. Buchleitner, and F. de Melo, Phys. Rev. A **79**, 032322 (2009).
[20] S. L. Zhang, X. B. Zou, S. Yang, C. F. Li, C. H. Jin, and G. C. Guo, Phys. Rev. A **80**, 062320 (2009).
[21] C. Genes, A. Mari, P. Tombesi, and D. Vitali, Phys. Rev. A **78**, 032316 (2008).
[22] M. O. Scully and M. S. Zubairy, *Quantum Optics* (Cambridge University Press, Cambridge, UK, 1997).
[23] D. Segal, Phys. Rev. E **77**, 021103 (2008).
[24] N. G. de Almeida, R. J. Napolitano, and M. H. Y. Moussa, Phys. Rev. A **62**, 33815 (2000).
[25] P. Marian and T. A. Marian, Phys. Rev. A **47**, 4474 (1993).
[26] L. Hu and H. Fan, Phys. Scr. **79**, 035004 (2009).
[27] J. Chen *et al.*, Mod. Appl. Sci. **3**, 36 (2009); P. S. An and G. G. Can, Sci Rep. **8**, 579 (1990).
[28] H.-P. Breuer and F. Petruccione, *The Theory of Open Quantum Systems* (Oxford University Press, New York, 2002).